

# Nonreciprocal enhancement of remote entanglement between nonidentical mechanical oscillators

Ya-Feng Jiao,<sup>1,2</sup> Ying Li,<sup>1</sup> Jing-Xue Liu,<sup>1</sup> Ronghua Yang,<sup>2</sup> Le-Man Kuang,<sup>1,3,\*</sup> and Hui Jing<sup>1,3,†</sup>

<sup>1</sup>*Key Laboratory of Low-Dimensional Quantum Structures and Quantum Control of Ministry of Education, Department of Physics and Synergetic Innovation Center for Quantum Effects and Applications, Hunan Normal University, Changsha 410081, China*

<sup>2</sup>*Laboratory of Chemical Biology & Traditional Chinese Medicine Research, Ministry of Education College of Chemistry and Chemical Engineering, Hunan Normal University, Changsha 410081, China*

<sup>3</sup>*Synergetic Innovation Academy for Quantum Science and Technology, Zhengzhou University of Light Industry, Zhengzhou 450002, China*

(Dated: August 23, 2022)

Entanglement between distinct massive mechanical oscillators is of particular interest in quantum-enabled devices due to its potential applications in quantum information processing. Here we propose how to achieve nonreciprocal remote entanglement between two spatially separated mechanical oscillators within a cascaded optomechanical configuration, where the two optomechanical resonators are indirectly coupled through a telecommunication fiber. We show that by selectively spinning the optomechanical resonators, one can break the time reversal symmetry of this compound system via Sagnac effect, and more excitingly, enhance the indirect couplings between distinct mechanical oscillators via the individual optimizations of light-motion interaction in each optomechanical resonator. This allows us to achieve nonreciprocal entanglement between distinct mechanical oscillators, that is, the generation of such entanglement can only be unidirectionally implemented through driving the system from one specific input direction but not the other. Moreover, in case of nonidentical mechanical oscillators, it is found that the degree of the generated nonreciprocal entanglement is counterintuitively enhanced in comparison with its reciprocal counterparts, which are otherwise inaccessible in static cascaded systems with a single-tone driving laser. Our work, which is well within the feasibility of current experimental capabilities, provides an enticing new opportunity to explore the nonclassical correlations between distinct massive objects and facilitates a variety of emerging quantum technologies ranging from quantum information processing to quantum sensing.

## I. INTRODUCTION

Entanglement, characterized by the abilities to explore strong nonclassical correlations between distinct quantum systems with spatial separation, is a peculiar feature of quantum physics [1]. When sharing entanglement between different components in a composite quantum system, it could provide key quantum resources for a variety of nascent quantum technologies ranging from quantum information processing [2, 3] to quantum sensing [4], leading to the advances of quantum-enabled devices over its classical counterparts [5]. So far, although the concepts of entanglement is still counterintuitive, it has been experimentally prepared, manipulated and utilized within a myriad of physical platforms involving both atomic-scale particles and macroscopic-scale objects [6–8], e.g., photons [9, 10], ions [11, 12], atomic ensembles [13–15], and superconducting circuits [16, 17]. Very recently, the generation of heralded entanglement between two <sup>87</sup>Rb atoms was even experimentally observed over fibre links with a length of 33 km [18]. Moreover, with the recent advances in the emerging field of cavity optomechanics (COM) [19–21], the explorations of macroscopic quantum effects have been extended into a domain of massive mechanical oscillators [22–27]. For example, after subtracting the classical noise, nonclassical correlations were even demonstrated

between light and 40 kg mirrors at room temperature [28]. In the past few years, thanks to the coherent light-motion interactions of COM systems [29], quantum entanglement have not only been intensively investigated and experimentally demonstrated between electromagnetic field and vibrational modes [30–35], as well as between propagating radiation fields [36–38] or massive mechanical oscillators [39–46]. Especially, by using multi-tone optical driving as an intermediary, the entangled state of distinct mechanical motions has been deterministically generated and directly observed with high fidelity in very recent experiments within optical or microwave COM systems [47–50].

In parallel to these advances, nonreciprocal optical devices, serving as pivotal fundamental components in the fields of photonic quantum information processing [51], have also attracted intense interests for their unique properties of unidirectional manipulation of light-matter interactions [52–54]. In the past few decades, by breaking the time-reversal symmetry, several schemes have been proposed and experimentally demonstrated to fabricate nonreciprocal optical devices, which are generally based on magnetic materials [55], atomic gases [56–58], optical or quantum nonlinearities [59–63], optomechanics [64–67], synthetic structures [68–71], and moving medium [72–74]. As a crucial element for engineering the propagation of light, nonreciprocal optical devices have a wide range of applications, including invisible cloaking [75], unidirectional lasing [76], and suppression of backscattering [77]. In recent years, nonreciprocal optical devices have also been extended to realize the one-way control of diverse physical phenomenon, such as optical chaos [78] or soli-

\* lmkuang@hunnu.edu.cn

† jinghui73@gmail.com

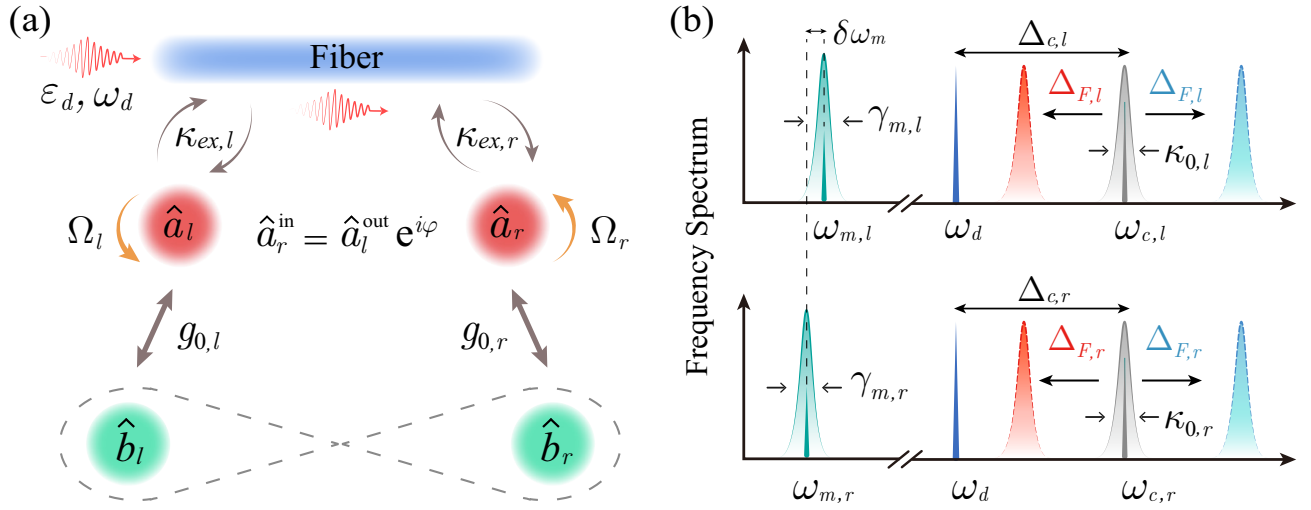


FIG. 1. (a) Schematic diagram of a unidirectional cascaded COM system composed of two spinning COM resonators and a telecommunication fiber. The two COM resonators are assumed to have neither direct acoustic interaction nor near-field optical couplings, and their indirect coupling is enabled by the light field propagating in the fiber. By selectively spinning the COM resonators and properly adjusting their spinning directions, the entanglement between the two spatially separated mechanical oscillators become direction-dependent, that is, it could be achieved when light is input from one specific direction but not the other. (b) Frequency spectrum of each spinning COM resonator. By spinning the COM resonators along CCW direction, we have  $\Delta_{F,j} > 0$  for the case of left input, while  $\Delta_{F,j} < 0$  for the case of right input.

tons [79], phonon [80] or magnon lasing [81], and optomechanical high-order sidebands [82]. These previous studies have mainly focused on the classical statistical properties of light rather than its quantum correlations, i.e., the unidirectional control of optical transmittance. In view of advances in chiral quantum optics [53], nonreciprocal quantum devices have also been pursued very recently, which provides an indispensable tool for achieving, e.g., single-photon isolator [83–85] or circulator [86, 87], unidirectional flow of thermal noise [88], and one-way photon [89–91] or magnon blockade [92]. Particularly, we note that by using spinning COM devices, nonreciprocal entanglement between optical field and mechanical motion was proposed in a recent study, which reveals a counterintuitive property of such nonreciprocal entangled states as being robust against random losses [93].

In this paper, we propose how to achieve nonreciprocal remote entanglement between two distinct mechanical oscillators in a cascaded COM system which is composed of two spinning COM resonators and a telecommunication fiber, unveiling its unique properties that are otherwise inaccessible within its reciprocal counterparts. Specifically, by selectively spinning the COM resonators and properly adjusting their spinning directions, we presented an effective method to generate and manipulate nonreciprocal entanglement between two mechanical oscillators. More excitingly, we found that in case of nonidentical mechanical oscillators, especially of those with frequency mismatch, the achievement of such nonreciprocal entanglement provides an enticing new opportunity to enhance its entanglement degree. The Sagnac effect induced by spinning devices played a key role in this process. It allowed us to break the time reversal symmetry of this compound system, and also to enhance the optical-radiation-pressure mediated couplings between mechanical oscillators

via the individual optimization of light-motion interaction in each COM resonator. These results are established with the parameters that are well within the feasibilities of current experimental capabilities. As such, we anticipate that our work could serve as a useful tool to explore the nonclassical natures of systems involving massive mechanical objects [39–50], open up promising new ways to engineer various quantum effect with diverse nonreciprocal devices [52–54], and provide crucial quantum resources to a large number of emerging quantum technologies ranging from quantum information processing to quantum sensing [21, 51].

## II. THEORETICAL MODEL AND DYNAMICS OF A CASCADED SPINNING COM SYSTEM

As studied in details in Refs [39–50], for two spatially separated mechanical objects, the macroscopic entanglement between them could be generated with the help of an optical-radiation-pressure mediated interaction. Meanwhile, it is shown that the emergence of such macroscopic entanglement by using a single-tone optical driving occurs only within a small bandwidth around the resonant mechanical parameter region [40], i.e., indicating that this scheme requires each mechanical oscillator with identical COM coupling rate, resonance frequency and damping rate. In terms of creating and detecting entanglement between non-identical mechanical oscillators, especially between those with mismatched fundamental frequencies, an effective approach is to apply a strategy that involves a multi-tone optical driving process [45], in which each tone of the multiplexing laser is assumed to be associated with a specific mechanical oscillator. Important experimental milestone researches toward this goal have been

reached very recently using pulsed multi-tone driving in optical or microwave COM systems [47–50]. However, the constraints on efficiencies of this multi-tone driving scheme, in comparison with its counterpart performed by a single-tone driving, are twofold: (i) the multi-tone driving scheme works optimally under the rotating wave approximation (RWA) condition [45], and thus it requires the fundamental mechanical frequencies  $\omega_m$  and the corresponding frequency difference  $\delta\omega_m$  to be much larger than the cavity bandwidth  $\kappa$ , i.e.,  $\omega_m, \delta\omega_m \gg \kappa$ ; (ii) applying additional driving lasers with distinct tones would impose additional input noises, which further inhibits the emergence of mechanical entanglement with ever greater entanglement degree. In the following discussion, the frequency mismatch  $\delta\omega_m$  is defined as  $\delta\omega_m/\omega_{m,l} = 1 - \chi$ , with a mechanical frequency ratio  $\chi = \omega_{m,r}/\omega_{m,l}$ . For current experimental techniques with optical cavities, it still remains a tough challenge to satisfy the above RWA condition for small values of  $\delta\omega_m$ , which requires ultra-high quality factors of cavity modes. Therefore, it is necessary to establish an alternative method to create and manipulate remote entanglement between non-identical mechanical oscillators.

In this paper, we propose how to achieve nonreciprocal remote entanglement between two massive mechanical oscillators, unveiling its unique properties that are otherwise unattainable within reciprocal systems. Specifically, as shown in Fig. 1, we consider a unidirectional cascaded COM system consisting of two spatially distant whispering-gallery-mode (WGM) resonators and a telecommunication fiber. The two WGM resonators are assumed to have neither direct acoustic interaction nor near-field optical couplings. By design, each WGM resonator could support a pair of localized optical and mechanical modes with fundamental frequencies  $\omega_{c,j}$  and  $\omega_{m,j}$ , respectively. Here the index,  $j = l, r$ , are referred to as the WGM resonator placed on the left- or right-hand side. Due to the optical-radiation-pressure interactions, the localized optical and mechanical modes could be coupled with each other. Furthermore, the input optical field in the fiber could be coupled into and out of the  $j$ -hand-side WGM resonator via evanescent couplings (with a coupling rate  $\kappa_{ex,j}$ ), and propagates between the two WGM resonators unidirectionally, thereby leading to an indirect inter-cavity coupling between the optical modes [94, 95]. Finally, we remark that by utilizing such cascaded configurations, frequency locking or synchronization of distant nano-mechanical oscillators has been experimentally demonstrated very recently [96, 97].

Based on this compound system, an effective way for achieving optical nonreciprocity is to break the time-reversal symmetry of this system through selectively spinning the WGM resonators [98]. For example, nonreciprocal transmission with 99.6% isolation was observed for light within a spinning WGM sphere in a recent experiment [74], without the facility of any magnetic materials, optical nonlinearities and complex spatial structures. In such spinning devices, counter-propagating lights experience different effective lengths of optical path as it travels for a whole closed loop, thus leading to an irreversible refractive index for the clockwise (CW) and counter-clockwise (CCW) modes [74],

that is,  $n_{\pm} = n[1 \pm nR\Omega(n^{-2} - 1)/c]$ , where  $n$  and  $\Omega$  are the refractive index and the angular velocity of a WGM resonator with radius  $R$ , respectively, and  $c$  is the speed of light in vacuum. Correspondingly, the degeneracy of the CW and CCW modes is lifted by a Fizeau frequency shift  $\Delta_F$ , resulting from the well-known Sagnac effect. As a result, by spinning the  $j$ -hand-side WGM resonator along the CCW direction, we have  $\Delta_{F,j} > 0$  ( $\Delta_{F,j} < 0$ ) for the case of left (right) input direction, and thus the effective resonance frequencies of the counter-propagating modes are given by,

$$\omega_{j,s} \equiv \omega_{c,j} \pm |\Delta_{F,j}|, \quad (1)$$

with  $s = \circlearrowleft, \circlearrowright$  indexing the CW or CCW optical modes, and

$$\Delta_{F,j} = \pm \Omega_j \frac{n_j R_j \omega_{c,j}}{c} \left( 1 - \frac{1}{n_j^2} - \frac{\lambda_j}{n_j} \frac{dn_j}{d\lambda_j} \right), \quad (2)$$

where  $\lambda_j = c/\omega_{c,j}$  is the wavelength of light in vacuum. The dispersion term  $dn_j/d\lambda_j$ , characterizing the relativistic origin of the Sagnac effect, is relatively small in typical materials (reaching up to  $\sim 1\%$ ) [74, 99].

In a rotating frame with respect to  $\hat{H}_d = \hbar\omega_d(\hat{a}_l^\dagger \hat{a}_l + \hat{a}_r^\dagger \hat{a}_r)$ , the Hamiltonian of this compound system, with each WGM resonator spinning along the CCW direction and the optical driving field input from the left-hand side, is given by

$$\begin{aligned} \hat{H} &= \hat{H}_0 + \hat{H}_{\text{int}} + \hat{H}_{\text{dr}}, \\ \hat{H}_0 &= \hbar\Delta_{l,\circlearrowleft}\hat{a}_l^\dagger \hat{a}_l + \hbar\Delta_{r,\circlearrowright}\hat{a}_r^\dagger \hat{a}_r + \hbar\omega_{m,l}\hat{b}_l^\dagger \hat{b}_l + \hbar\omega_{m,r}\hat{b}_r^\dagger \hat{b}_r, \\ \hat{H}_{\text{int}} &= -\hbar g_{0,l}\hat{a}_l^\dagger \hat{a}_l(\hat{b}_l^\dagger + \hat{b}_l) - \hbar g_{0,r}\hat{a}_r^\dagger \hat{a}_r(\hat{b}_r^\dagger + \hat{b}_r), \\ \hat{H}_{\text{dr}} &= i\hbar\sqrt{\kappa_{ex,l}}\varepsilon_d(\hat{a}_l^\dagger - \hat{a}_l), \end{aligned} \quad (3)$$

where  $\hat{a}_j$  ( $\hat{a}_j^\dagger$ ) and  $\hat{b}_j$  ( $\hat{b}_j^\dagger$ ) are, respectively, the optical and mechanical annihilation (creation) operators, and  $\Delta_{j,\circlearrowleft} = \omega_{j,\circlearrowleft} - \omega_d$  denotes the optical detuning between the spinning resonator and the driving field. The corresponding frame rotating with driving frequency  $\omega_d$  was implemented by applying a unitary transformation, i.e.,  $\hat{H} = \hat{U}\hat{H}_{\text{old}}\hat{U}^\dagger - i\hbar\hat{U}\partial\hat{U}^\dagger/\partial t$ , with  $\hat{U} = \exp[i\hat{H}_d t/\hbar]$  (see, e.g., Refs. [19] for more details). The parameter  $g_{0,j} = (\omega_{c,j}/R_j)\sqrt{\hbar/m_j\omega_{m,j}}$  denotes the single-photon COM coupling strength of the  $j$ -hand-side WGM resonator, with an effective mass  $m_j$ . The field amplitude of the driving laser is given by  $|\varepsilon_d| = \sqrt{P_d/\hbar\omega_d}$ , and  $P_d$  is referred to as the input laser power of the driving field. Note that for studying the case where the driving field is input from right-hand side, one should alter the index of the optical detuning, i.e.,  $\Delta_{j,\circlearrowleft} \rightarrow \Delta_{j,\circlearrowright}$ , and change the Hamiltonian of the driving field to  $\hat{H}_{\text{dr}} = i\hbar\sqrt{\kappa_{ex,r}}\varepsilon_d(\hat{a}_r^\dagger - \hat{a}_r)$ .

In the following discussions, as a specific example, we focus on the left-hand-side driving case and show how to explore the dynamics of this compound system. By introducing dissipations and input noises, the equations of motion for arbitrary optical and mechanical operators could be obtained through employing the quantum Langevin equations (QLEs), which

are given by

$$\begin{aligned}\dot{\hat{a}}_l &= -\left(i\Delta_{l,\circ} + \frac{\kappa_{0,l} + \kappa_{ex,l}}{2}\right)\hat{a}_l + ig_{0,l}\hat{a}_l(\hat{b}_l^\dagger + \hat{b}_l) \\ &\quad + \sqrt{\kappa_{ex,l}}\varepsilon_d + \sqrt{\kappa_{0,l}}\hat{a}_{0,l}^\text{in} + \sqrt{\kappa_{ex,l}}\hat{a}_{ex,l}^\text{in}, \\ \dot{\hat{a}}_r &= -\left(i\Delta_{r,\circ} + \frac{\kappa_{0,r} + \kappa_{ex,r}}{2}\right)\hat{a}_r + ig_{0,r}\hat{a}_r(\hat{b}_r^\dagger + \hat{b}_r) \\ &\quad + \sqrt{\eta\kappa_{ex,r}}\hat{a}_{f,r}^\text{in} + \sqrt{\kappa_{0,r}}\hat{a}_{0,r}^\text{in} + \sqrt{\kappa_{ex,r}}\hat{a}_{ex,r}^\text{in}, \\ \dot{\hat{b}}_l &= -\left(i\omega_{m,l} + \frac{\gamma_{m,l}}{2}\right)\hat{b}_l + ig_{0,l}\hat{a}_l^\dagger\hat{a}_l + \sqrt{\gamma_{m,l}}\hat{b}_l^\text{in}, \\ \dot{\hat{b}}_r &= -\left(i\omega_{m,r} + \frac{\gamma_{m,r}}{2}\right)\hat{b}_r + ig_{0,r}\hat{a}_r^\dagger\hat{a}_r + \sqrt{\gamma_{m,r}}\hat{b}_r^\text{in},\end{aligned}\quad (4)$$

where  $\kappa_{0,j}$  and  $\gamma_{m,j}$  are the intrinsic decay rates of the optical and mechanical modes, respectively.  $\hat{a}_{0,j}^\text{in}$  and  $\hat{a}_{ex,j}^\text{in}$  describe two distinct types of Gaussian noise caused by the zero point fluctuations of optical field from vacuum and fiber mode, whereas  $\hat{b}_j^\text{in}$  denotes the input vacuum noise operators for the mechanical modes. These input vacuum noise operators have zero mean values and are characterized by the following correlation functions [100]:

$$\begin{aligned}\left\langle \hat{a}_{0,j}^\text{in}(t)\hat{a}_{0,j'}^\text{in,\dagger}(t') \right\rangle &= \delta_{jj'}\delta(t-t'), \\ \left\langle \hat{a}_{ex,j}^\text{in}(t)\hat{a}_{ex,j'}^\text{in,\dagger}(t') \right\rangle &= \delta_{jj'}\delta(t-t'), \\ \left\langle \hat{b}_j^\text{in}(t)\hat{b}_{j'}^\text{in,\dagger}(t') \right\rangle &= (\bar{n}_{m,j} + 1)\delta_{jj'}\delta(t-t'), \\ \left\langle \hat{b}_j^\text{in,\dagger}(t)\hat{b}_{j'}^\text{in}(t') \right\rangle &= \bar{n}_{m,j}\delta_{jj'}\delta(t-t'),\end{aligned}\quad (5)$$

where  $\bar{n}_{m,j} = [\exp(\hbar\omega_{m,j}/k_B T) - 1]^{-1}$  is the thermal mean occupation number of the memecanical mode,  $k_B$  is the Boltzmann constant, and  $T$  is the bath temperature of the mechanical mode. Here we have assumed that the cavity modes are in ordinary zero-temperature environments, whereas the mechanical modes are surrounded by thermal reservoirs. In addition, the operator  $\hat{a}_{f,r}^\text{in}$  denotes the coherent input optical field of the right-hand-side WGM resonator. Based on the properties of cascaded systems [94–97] and the input-output relations, we have

$$\begin{aligned}\hat{a}_{f,r}^\text{in} &= \hat{a}_l^\text{out}e^{i\varphi}, \\ \hat{a}_l^\text{out} &= \varepsilon_d - \sqrt{\kappa_{ex,l}}\hat{a}_l,\end{aligned}\quad (6)$$

where the additional phase  $\varphi$  describes the accumulated phase delay resulting from light propagation between the two spinning WGM resonators, and it is given by

$$\varphi \equiv \omega_d\tau = 2\pi \frac{nL}{\lambda},\quad (7)$$

where  $\tau$  denotes the propagating time, and  $L$  is the length of the fiber between the coupling regions of the two WGM resonators. Moreover,  $\eta \in [0, 1]$  represents the power transmission coefficient of the propagating field in the fiber, which accounts for the imperfect couplings between the two spinning WGM resonators. For  $\eta = 1$ , it indicates the case of a lossless unidirectional coupling, and in contrast,  $\eta = 0$  corresponds

to the situation where the two spinning WGM resonators are independent without any optical coupling.

The QLEs (4) involves the radiation-pressure induced nonlinear COM interactions between optical fields and mechanical oscillators, and thus it is difficult to be directly solved. In order to find solutions to such set of nonlinear dynamical equations, one can expand each operator as a sum of its steady-state mean value and a small quantum fluctuation around it under the condition of strong optical driving. By substituting  $\hat{a}_j = \alpha_j + \delta\hat{a}_j$  for the optical field and  $\hat{b}_j = \beta_j + \delta\hat{b}_j$  for the mechanical mode into Eq. (4), we obtain the following first-order inhomogeneous differential equations for steady-state mean values

$$\begin{aligned}\dot{\alpha}_l &= -\left(i\tilde{\Delta}_{l,\circ} + \frac{\kappa_{0,l} + \kappa_{ex,l}}{2}\right)\alpha_l + \sqrt{\kappa_{ex,l}}\varepsilon_d, \\ \dot{\alpha}_r &= -\left(i\tilde{\Delta}_{r,\circ} + \frac{\kappa_{0,r} + \kappa_{ex,r}}{2}\right)\alpha_r - \sqrt{\eta\kappa_{ex,l}\kappa_{ex,r}}e^{i\varphi}\alpha_l \\ &\quad + \sqrt{\eta\kappa_{ex,r}}e^{i\varphi}\varepsilon_d, \\ \dot{\beta}_l &= -\left(i\omega_{m,l} + \frac{\gamma_{m,l}}{2}\right)\beta_l + ig_{0,l}|\alpha_l|^2, \\ \dot{\beta}_r &= -\left(i\omega_{m,r} + \frac{\gamma_{m,r}}{2}\right)\beta_r + ig_{0,r}|\alpha_r|^2,\end{aligned}\quad (8)$$

and the corresponding linearized QLEs for quantum fluctuations

$$\begin{aligned}\delta\dot{\hat{a}}_l &= -\left(i\tilde{\Delta}_{l,\circ} + \frac{\kappa_{0,l} + \kappa_{ex,l}}{2}\right)\delta\hat{a}_l + ig_{0,l}\alpha_l(\delta\hat{b}_l^\dagger + \delta\hat{b}_l) \\ &\quad + \sqrt{\kappa_{0,l}}\hat{a}_{0,l}^\text{in} + \sqrt{\kappa_{ex,l}}\hat{a}_{ex,l}^\text{in}, \\ \delta\dot{\hat{a}}_r &= -\left(i\tilde{\Delta}_{r,\circ} + \frac{\kappa_{0,r} + \kappa_{ex,r}}{2}\right)\delta\hat{a}_r - \sqrt{\eta\kappa_{ex,l}\kappa_{ex,r}}e^{i\varphi}\delta\hat{a}_l \\ &\quad + ig_{0,r}\alpha_r(\delta\hat{b}_r^\dagger + \delta\hat{b}_r) + \sqrt{\kappa_{0,r}}\hat{a}_{0,r}^\text{in} + \sqrt{\kappa_{ex,r}}\hat{a}_{ex,r}^\text{in}, \\ \dot{\delta\hat{b}}_l &= -\left(i\omega_{m,l} + \frac{\gamma_{m,l}}{2}\right)\delta\hat{b}_l + ig_{0,l}(\alpha_l\delta\hat{a}_l^\dagger + \alpha_l^*\delta\hat{a}_l) \\ &\quad + \sqrt{\gamma_{m,l}}\hat{b}_l^\text{in}, \\ \dot{\delta\hat{b}}_r &= -\left(i\omega_{m,r} + \frac{\gamma_{m,r}}{2}\right)\delta\hat{b}_r + ig_{0,r}(\alpha_r\delta\hat{a}_r^\dagger + \alpha_r^*\delta\hat{a}_r) \\ &\quad + \sqrt{\gamma_{m,r}}\hat{b}_r^\text{in},\end{aligned}\quad (9)$$

where  $\tilde{\Delta}_{j,\circ} = \Delta_{c,j} + |\Delta_{F,j}|$ , and  $\Delta_{c,j} = (\omega_{c,j} - \omega_d) - g_{0,j}(\beta_j^* + \beta_j)$  is an effective optical detuning caused by radiation-pressure mediated phase shift. By setting all derivatives in Eq. (8) to be zero, the steady-state mean values of the optical and mechanical modes can be obtained as

$$\begin{aligned}\alpha_l &= \frac{\sqrt{\kappa_{ex,l}}\varepsilon_d}{i\tilde{\Delta}_{l,\circ} + (\kappa_{0,l} + \kappa_{ex,l})/2}, \\ \alpha_r &= \frac{\sqrt{\eta\kappa_{ex,r}}e^{i\varphi}(\varepsilon_d - \sqrt{\kappa_{ex,l}}\alpha_l)}{i\tilde{\Delta}_{r,\circ} + (\kappa_{0,r} + \kappa_{ex,r})/2}, \\ \beta_j &= \frac{ig_{0,j}|\alpha_j|^2}{i\omega_{m,j} + \gamma_{m,j}/2}.\end{aligned}\quad (10)$$

Equation (10) indicates that the intracavity photon number,  $N_j \equiv |\alpha_j|^2$ , of the left-hand-side WGM resonator is merely related to the pump strength of the input driving field and,

simultaneously, it also dominates the intracavity photon number of the right-hand-side WGM resonator. In addition, it is clearly seen that although the field amplitude of the right-hand-side COM resonator is associated with the propagating phase delay  $\varphi$ , the intracavity photon number of such WGM resonator is independent of it, implying that the effective COM coupling strength of the right-hand-side COM resonator is identical for arbitrary propagating distance in lossless unidirectional cascaded COM systems.

By defining the optical and mechanical quadrature fluctuation operators as

$$\begin{aligned}\hat{X}_j &= \frac{1}{\sqrt{2}}(\delta\hat{a}_j^\dagger + \delta\hat{a}_j), \quad \hat{Y}_j = \frac{i}{\sqrt{2}}(\delta\hat{a}_j^\dagger - \delta\hat{a}_j), \\ \hat{q}_j &= \frac{1}{\sqrt{2}}(\delta\hat{b}_j^\dagger + \delta\hat{b}_j), \quad \hat{p}_j = \frac{i}{\sqrt{2}}(\delta\hat{b}_j^\dagger - \delta\hat{b}_j),\end{aligned}\quad (11)$$

and the associated Hermitian input noise operators as

$$\begin{aligned}\hat{x}_j^{\text{in}} &= \frac{1}{\sqrt{2}}(\hat{a}_j^{\text{in}\dagger} + \hat{a}_j^{\text{in}}), \quad \hat{y}_j^{\text{in}} = \frac{i}{\sqrt{2}}(\hat{a}_j^{\text{in}\dagger} - \hat{a}_j^{\text{in}}), \\ \hat{q}_j^{\text{in}} &= \frac{1}{\sqrt{2}}(\hat{b}_j^{\text{in}\dagger} + \hat{b}_j^{\text{in}}), \quad \hat{p}_j^{\text{in}} = \frac{i}{\sqrt{2}}(\hat{b}_j^{\text{in}\dagger} - \hat{b}_j^{\text{in}}),\end{aligned}\quad (12)$$

the corresponding linearized QLEs could be obtained in a compact form, i.e.,

$$\partial_t \hat{u} = A\hat{u}(t) + \hat{v}(t). \quad (13)$$

Here we have introduced the vector of quadrature fluctuation operators  $\hat{u} = (\hat{X}_l, \hat{Y}_l, \hat{X}_r, \hat{Y}_r, \hat{q}_l, \hat{p}_l, \hat{q}_r, \hat{p}_r)^T$ , the vector of input noise operator  $\hat{v} = (\hat{X}_l^{\text{in}}, \hat{Y}_l^{\text{in}}, \hat{X}_r^{\text{in}}, \hat{Y}_r^{\text{in}}, \sqrt{\gamma_{m,l}}\hat{q}_l^{\text{in}}, \sqrt{\gamma_{m,l}}\hat{p}_l^{\text{in}}, \sqrt{\gamma_{m,r}}\hat{q}_r^{\text{in}}, \sqrt{\gamma_{m,r}}\hat{p}_r^{\text{in}})^T$ , and the corresponding coefficient matrix

$$A = \begin{pmatrix} -\frac{\Gamma_l}{2} & \tilde{\Delta}_{l,\circ} & 0 & 0 & -\Lambda_l^{\text{im}} & 0 & 0 & 0 \\ -\tilde{\Delta}_{l,\circ} & -\frac{\Gamma_l}{2} & 0 & 0 & \Lambda_l^{\text{re}} & 0 & 0 & 0 \\ -J_c & J_s & -\frac{\Gamma_r}{2} & \tilde{\Delta}_{r,\circ} & 0 & 0 & -\Lambda_r^{\text{im}} & 0 \\ -J_s & -J_c & -\tilde{\Delta}_{r,\circ} & -\frac{\Gamma_r}{2} & 0 & 0 & \Lambda_r^{\text{re}} & 0 \\ 0 & 0 & 0 & 0 & -\frac{\gamma_{m,l}}{2} & \omega_{m,l} & 0 & 0 \\ \Lambda_l^{\text{re}} & \Lambda_l^{\text{im}} & 0 & 0 & -\omega_{m,l} & -\frac{\gamma_{m,l}}{2} & 0 & 0 \\ 0 & 0 & 0 & 0 & 0 & -\frac{\gamma_{m,r}}{2} & \omega_{m,r} & 0 \\ 0 & 0 & \Lambda_r^{\text{re}} & \Lambda_r^{\text{im}} & 0 & 0 & -\omega_{m,r} & -\frac{\gamma_{m,r}}{2} \end{pmatrix} \quad (14)$$

with the following components

$$\begin{aligned}\hat{X}_j^{\text{in}} &= \sqrt{\kappa_{0,j}}\hat{x}_{0,j}^{\text{in}} + \sqrt{\kappa_{ex,j}}\hat{x}_{ex,j}^{\text{in}}, \\ \hat{Y}_j^{\text{in}} &= \sqrt{\kappa_{0,j}}\hat{y}_{0,j}^{\text{in}} + \sqrt{\kappa_{ex,j}}\hat{y}_{ex,j}^{\text{in}}, \\ \Gamma_j &= \kappa_{0,j} + \kappa_{ex,j}, \\ \Lambda_j^{\text{re}} &= 2g_j \text{Re}[\alpha_j], \quad \Lambda_j^{\text{im}} = 2g_j \text{Im}[\alpha_j], \\ J_s &= \sqrt{\eta\kappa_{ex,l}\kappa_{ex,r}} \sin \varphi, \quad J_c = \sqrt{\eta\kappa_{ex,l}\kappa_{ex,r}} \cos \varphi.\end{aligned}\quad (15)$$

The solution of the linearized QLEs (13) is given by  $\hat{u}(t) = \mathcal{M}(t)\hat{u}(0) + \int_0^t ds \mathcal{M}(s)\hat{v}(t-s)$ , where  $\mathcal{M} = \exp(At)$ . If all real parts of the eigenvalues of  $A$  are negative, the system is stable and could reach its steady state, which is determined by the Routh-Hurwitz criterion [101]. When all the stability condition is satisfied, we could obtain  $\mathcal{M}(\infty) = 0$  in the steady state and

$$\hat{u}_i(\infty) = \int_0^\infty ds \sum_k \mathcal{M}_{ik}(s)\hat{v}_k(t-s). \quad (16)$$

Due to the linearized dynamics of the quantum fluctuation quadratures and the Gaussian nature of the input noises, the steady state of this compound system, independently of any initial conditions, could finally evolve into a zero mean quadripartite Gaussian state, which allows us to characterize its steady-state properties by an  $8 \times 8$  covariance matrix (CM)  $V$ , with the matrix elements defined as

$$V_{kl} = \langle \hat{u}_k(\infty)\hat{u}_l(\infty) + \hat{u}_l(\infty)\hat{u}_k(\infty) \rangle / 2 \quad (k, l = 1, 2, \dots, 8). \quad (17)$$

By using the steady-state solutions in Eq. (16) and the fact that the eight components of  $\hat{v}(t)$  are uncorrelated with each other, one gets

$$V = \int_0^\infty ds \mathcal{M}(s) D \mathcal{M}^T(s), \quad (18)$$

where  $D = (1/2) \text{Diag}[\Gamma_l, \Gamma_l, \Gamma_r, \Gamma_r, \gamma_{m,l}(2\bar{n}_{m,l}+1), \gamma_{m,l}(2\bar{n}_{m,l}+1), \gamma_{m,r}(2\bar{n}_{m,r}+1), \gamma_{m,r}(2\bar{n}_{m,r}+1)]$  is the diffusion matrix, and it is defined through  $D_{kl}\delta(s-s') = \langle \hat{v}_k(s)\hat{v}_l(s') + \hat{v}_l(s')\hat{v}_k(s) \rangle / 2$ . When the stability condition is fulfilled, the steady-state CM  $V$  in Eq. (18) is determined by the following Lyapunov equation

$$AV + VA^T = -D. \quad (19)$$

Clearly, it is seen that the Lyapunov equation (19) is linear for  $V$  and could be solved straightforwardly, thereby implying that one can derive the CM  $V$  for any specific value of relevant parameters.

### III. NONRECIPROCAL REMOTE ENTANGLEMENT BETWEEN TWO MECHANICAL OSCILLATORS

In order to quantify the bipartite entanglement of a multimode continuous variable (CV) system, one can adopt the logarithmic negativity  $E_{\mathcal{N}}$  as an effective measure, which is defined as [102]

$$E_{\mathcal{N}} = \max [0, -\ln(2\nu^-)], \quad (20)$$

, where  $\nu^- = 2^{-1/2} \{ \Sigma(V_{\mu\nu}) - [\Sigma(V_{\mu\nu})^2 - 4 \det V_{\mu\nu}]^{1/2} \}^{1/2}$  (with  $\Sigma(V_{\mu\nu}) \equiv \det \mathcal{A} + \det \mathcal{B} - 2 \det \mathcal{C}$ ) is the minimum symplectic eigenvalue of the partial transpose of a reduced  $4 \times 4$  CM,  $V_{\mu\nu}$ , with  $\mu$  and  $\nu$  describing the two selected modes under consideration. The reduced CM  $V_{\mu\nu}$  contains the entries of  $V$  associated with the corresponding bipartition  $\mu$  and  $\nu$ , which can be obtained straightforwardly by tracing out the rows and columns of the uninteresting modes in  $V$ . By writing the reduced CM  $V_{\mu\nu}$  in a  $2 \times 2$  block form, we have

$$V_{\mu\nu} = \begin{pmatrix} \mathcal{A} & \mathcal{C} \\ \mathcal{C}^T & \mathcal{B} \end{pmatrix}. \quad (21)$$

Note that the physicality of the reduced CM  $V_{\mu\nu}$  could be thoroughly checked by considering the fulfillment of the Heisenberg-Robinson uncertainty principle, that is, checking whether if the minimum symplectic eigenvalue  $\nu^-$  satisfies the condition that  $|\nu^-| \geq 1/2$ . In terms of the case with  $|\nu^-| < 1/2$ , the corresponding bipartition of

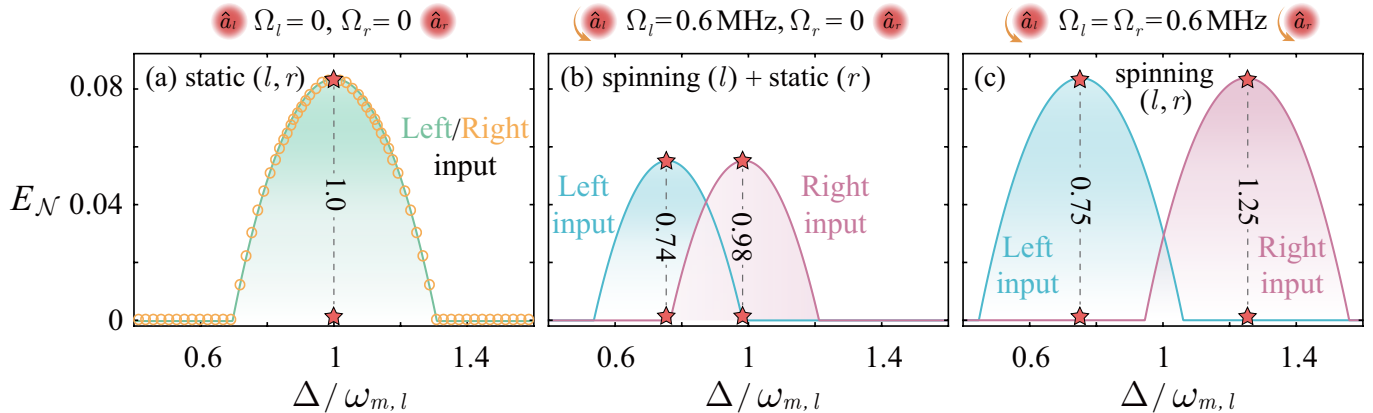


FIG. 2. Nonreciprocal remote entanglement between two identical mechanical oscillators. The logarithmic negativity  $E_N$  are plotted as a function of the scaled optical detuning  $\Delta/\omega_{m,l}$  for different input directions, with angular velocities of the left- and right-hand side WGM resonators (a)  $\Omega_l = 0$ ,  $\Omega_r = 0$ , (b)  $\Omega_l = 0.6$  MHz,  $\Omega_r = 0$ , and (c)  $\Omega_l = \Omega_r = 0.6$  MHz. In terms of the static case (i.e.,  $\Omega_l = \Omega_r = 0$ ),  $E_N$  is present only within a small interval around the resonance  $\Delta/\omega_{m,l} \simeq 1$  and keeps reciprocal for the opposite input directions. In contrast, for the spinning case (i.e.,  $\Omega_l \neq 0$  or  $\Omega_r \neq 0$ ), the resonance frequencies of the counterpropagating modes experience an opposite frequency shift due to the Sagnac effect, thereby leading to the peaks of  $E_N$  shifted for the opposite input directions.

the considered system gets entangled, which is equivalent to Simon's necessary and sufficient entanglement nonpositive partial transpose criterion (or the related Peres-Horodecki criterion) for certifying bipartite entanglement in Gaussian states [103]. Correspondingly, the logarithmic negativity,  $E_N$ , quantifying the amount by which the Peres-Horodecki criterion is violated, is an efficient measure that is widely used for certifying bipartite entanglement in CV systems.

In the following discussions, we first demonstrate how to achieve nonreciprocal remote entanglement between two identical mechanical oscillators (i.e.,  $\delta\omega_m = 0$  or  $\chi = 1$ ). Specifically, as shown in Fig. 2, the logarithmic negativity  $E_N$  for opposite input directions is plotted as a function of the scaled optical detuning  $\Delta/\omega_{m,l}$  with respect to different angular velocities of the two WGM resonators. In our numerical simulations, for ensuring the stability of this compound system, we assume that the following experimentally feasible parameters are employed for two identical WGM resonators [65, 74]:  $n = 1.48$ ,  $m = 15$  ng,  $R = 36$   $\mu\text{m}$ ,  $\lambda = 780$  nm,  $\kappa_0/2\pi = 15$  MHz,  $\omega_m/2\pi = 88.54$  MHz,  $\gamma_m/2\pi = 2.2$  kHz,  $P = 20$  mW,  $T = 100$  mK,  $\varphi = 0$ ,  $\eta = 1$ , and  $\Omega = 0.6$  MHz. Also, the fiber-cavity coupling rates for the left- and right-hand side WGM resonators are chosen as  $\kappa_{ex,l}/2\pi = 27$  MHz and  $\kappa_{ex,r}/2\pi = 30$  MHz, respectively. Moreover, due to the fact that the radiation-pressure induced frequency shift is much smaller than the cavity-pump detuning, i.e.,  $g_{0,j}(\beta_j^* + \beta_j) \ll |\omega_c - \omega_d|$ , we have already set  $\Delta_{c,l} = \Delta_{c,r} = \Delta$  for simplicity.

In case of static cascaded systems (i.e.,  $\Omega_l = \Omega_r = 0$ ), as shown in Fig. 2(a),  $E_N$  is present only within small interval of  $\Delta$  around the COM resonance  $\Delta/\omega_{m,l} = 1$ . Besides, it is also seen that  $E_N$  keeps reversible when switching the driving directions under the same parameter conditions [see solid and circle lines in Fig. 2(a)], which implies that the generation of the entanglement between mechanical oscillators is reciprocal for static cascaded systems. In contrast, as shown in Fig. 2(b), by spinning one arbitrary WGM resonator in this compound system (e.g.,  $\Omega_l \neq 0$  and  $\Omega_r = 0$ ),  $E_N$  becomes irreversible in regards of light input from opposite driving directions, indicating the achievement of nonreciprocal entanglement of the associated mechanical oscillators. This result implies that when a driving field with a specific frequency is applied to this compound system, one can entangle the two mechanical oscillators through the

radiation-pressure-induced interactions with respect to one specific input direction, whereas no entanglement could occur under the same parameter conditions for an opposite input direction [see  $E_N$  for different driving directions at e.g.,  $\Delta/\omega_{m,l} = 0.74$  or  $0.98$  in Fig. 2(b)]. However, it is also seen that the degree of such nonreciprocal entanglement is suppressed in comparison with the static situation. In addition, as shown in Fig. 2(c), it is found that in case of two WGM resonators spinning along the same direction,  $E_N$  could also be irreversible for opposite driving directions, which provides an alternative way to achieve such nonreciprocal entanglement. Besides, compared with the former case of a single spinning resonator, the generated entanglement in this situation acquires a higher entanglement degree, which is the same as that of a static system. In regards to two oppositely spinning WGM resonators, we have also confirmed that the generation of such entanglement is reversible due to the unbroken of time-reversal symmetry, and thus these results will not be reported here. The underlying physics for the generation of nonreciprocal entanglement can be understood as follows: In static cascaded systems, light experiences the same travel time and shares the same resonant wavelength with respect to the left and right input directions, which is guaranteed by the time-reversal symmetry of this compound system. Correspondingly, the optical-radiation-pressure mediated generation of the entanglement between mechanical oscillators is reciprocal in this regime. However, by selectively spinning the WGM resonators and properly adjusting their spinning directions, the time-reversal symmetry of this compound system is thus broken due to the presence of Sagnac effect. In this situation, the resonant wavelength becomes irreversible for opposite driving directions, which further results in the direction-dependent COM interactions for each WGM resonator. Therefore, for driving light with a specific wavelength, it could be observed that the generation of such optical-radiation-pressure mediated entanglement is nonreciprocal.

In Fig. 3, we further show the unique properties of nonreciprocal entanglement by which one can enhance the entanglement degree between two frequency-mismatched mechanical oscillators, thereby providing an enticing new opportunity to efficiently generate, manipulate and exploit entangled states of nonidentical mechanical objects at a wide range of frequencies. Figure 3(a) shows that, in case of a static cascaded system driven by a single-tone laser,  $E_N$  achieves

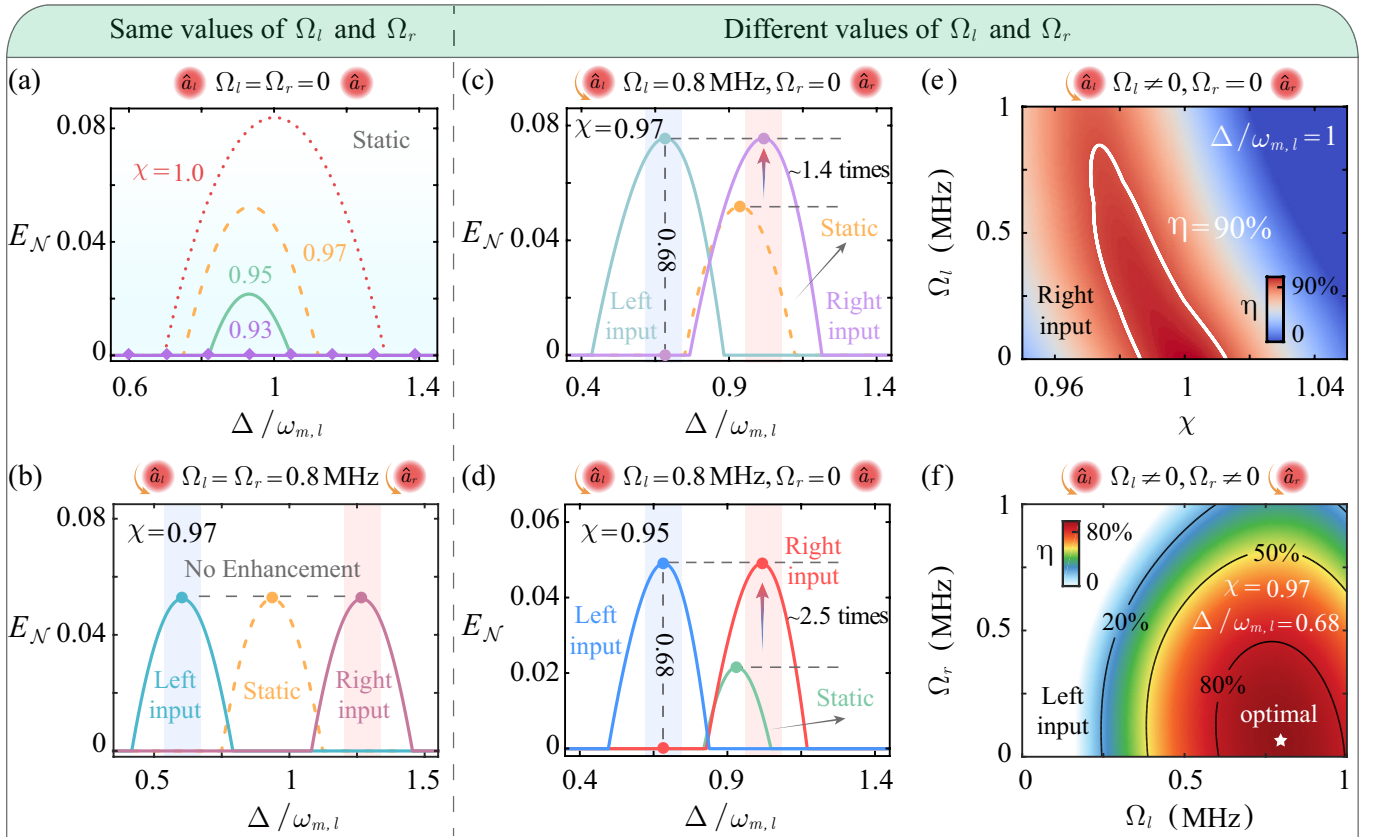


FIG. 3. Suppression of remote entanglement between two nonidentical mechanical oscillators due to their frequency mismatch, and its nonreciprocal revival resulting from the rotation induced compensation. The logarithmic negativity  $E_N$  are plotted as function of the scaled optical detuning  $\Delta/\omega_{m,l}$  for different input directions, with angular velocities of the left- and right-hand side WGM resonators (a)  $\Omega_l = \Omega_r = 0$ , (b)  $\Omega_l = \Omega_r = 0.8$  MHz, and (c)-(d)  $\Omega_l = 0.8$  MHz,  $\Omega_r = 0$ . For static cascaded systems,  $E_N$  tends to be inhibited as the mechanical frequency ratio  $\chi$  increases. In comparison, by spinning one of the WGM resonators, the maximum value of  $E_N$  could be enhanced for  $\sim 1.4$  or  $2.5$  times with respect to  $\chi = 0.97$  or  $0.95$ , almost reaching up to the values of the case with identical mechanical frequencies. (e) Density plot of the revival factor  $\eta$  as a function of the mechanical frequency ratio  $\chi$  and the angular velocity  $\Omega_l$ , with light input from right-hand side,  $\Omega_r = 0$  and  $\Delta/\omega_{m,l} = 1$ . (f) Density plot of the revival factor  $\eta$  as a function of the angular velocities  $\Omega_l$  and  $\Omega_r$ , with light input from left-hand side,  $\eta = 0.97$  and  $\Delta/\omega_{m,l} = 0.68$ .

its maximum value just at the mechanical frequency resonance, i.e.,  $\chi = 1$ , which is consistent with the results as shown in Ref. [40]. This result means that such mechanical entanglement tends to be inhibited or even vanished when one increases the frequency mismatch between the associated mechanical oscillators. For recent theoretical and experimental studies [45, 47–50], an effective approach for entangling two frequency-mismatched mechanical oscillators is to apply a multi-tone driving laser, where each tone of the driving laser is associated with a specific mechanical oscillator to generate correlations between them. However, the multi-tone driving scheme is generally restrained by the RWA approximation [45], which requires the fundamental mechanical frequencies  $\omega_m$  and the corresponding frequency difference  $\delta\omega_m$  to be much larger than the cavity bandwidth  $\kappa$ , i.e.,  $\omega_m, \delta\omega_m \gg \kappa$ . As a result, to fulfill this parameter condition of the RWA approximation, it usually requires ultra-high optical quality factors and large frequency difference of the associated mechanical oscillators. However, based on optical-wavelength microcavities, it still remains challenging for current experimental techniques to fabricate the COM devices with such characteristics. Here we further study how to entangle such two nonidentical mechanical oscillators by nonreciprocal control. As shown in Fig. 3(b),

by spinning the two WGM resonators along the same directions, it is seen that although the nonreciprocal entanglement could also be generated in this situation, the entanglement degree is not enhanced. However, as shown in Figs. 3(c) and 3(d), by spinning one arbitrary WGM resonator (e.g.,  $\Omega_l \neq 0$  and  $\Omega_r = 0$ ), it is found that the maximum values of  $E_N$  are considerably improved for one specific input direction in this cascaded spinning system, surpassing approximately an  $1.4$  or  $2.5$  times enhancement in degree of entanglement of that for the static case, while for the opposite input direction,  $E_N$  is correspondingly inhibited. These results can be understood as follows: For static cascaded systems, due to the frequency mismatch of the two mechanical oscillators, COM resonance condition is fulfilled merely by one specific WGM resonator with respect to the single-tone driving laser. Consequently, the effective interaction between the two mechanical oscillators is suppressed, which further leads to an inhibition of the optical-radiation-pressure mediated entanglement generation. In contrast, by means of selectively spinning the WGM resonators, the corresponding COM resonance condition is separately optimized for each WGM resonator, which provides facilities to the enhancement of such entanglement. In order to further quantify the amount by which the entanglement degree is enhanced,

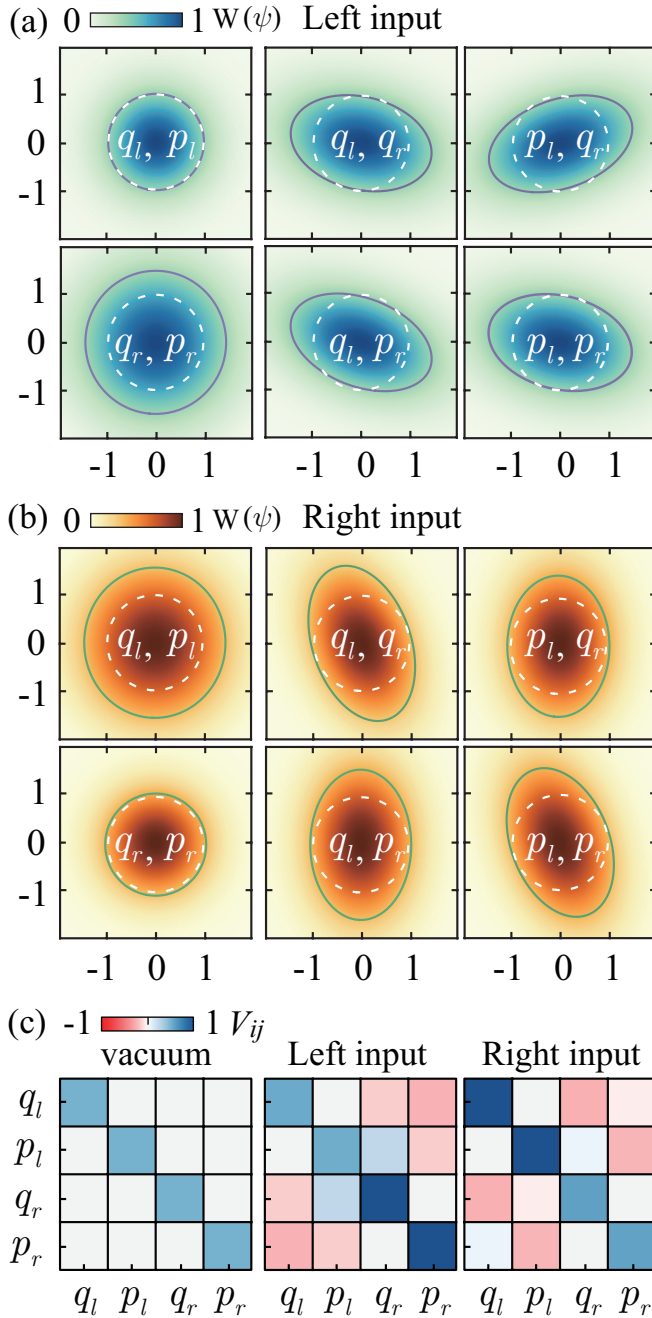


FIG. 4. Nonreciprocal quadrature statistics of two nonidentical mechanical oscillators in cascaded spinning COM systems. (a), (b) Reconstructed Wigner function  $W(\psi)$  for the steady state of the associated mechanical oscillators, with respect to the case where driving field is input from left- and right-hand side, respectively, along with that of an ideal vacuum state for reference. Each panel is corresponding to a characteristic projection of  $W(\psi)$  on two-dimensional subspaces within  $\psi = (q_l, p_l, q_r, p_r)^T$ , which is obtained by integrating out the other two quadratures in  $\psi$ . The solid (dashed) line indicates a drop by  $1/e$  of the maximum value of  $W(\psi)$  for the relevant steady (vacuum) state. The legends  $\psi_i, \psi_j$  in each panel are corresponding to a correlation with  $\psi_i$  along the x axis and  $\psi_j$  along the y axis. (c) Reduced CM  $V_{\mu\nu}$  of the two mechanical oscillators, which is associated with the CM used in (a) and (b). We set the optical detuning  $\Delta/\omega_{m,l} = 0.68$  and the mechanical frequency ratio  $\chi = 0.95$ . The other parameters are chosen as the same in the main text.

we define the following revival coefficient:

$$\eta = \frac{\max[E_N(\Omega \neq 0, \delta\omega \neq 0)]}{\max[E_N(\Omega = 0, \delta\omega = 0)]}. \quad (22)$$

As clearly seen in Figs. 3(e) and 3(f), the revival coefficient  $\eta$  could even reach up to the values above 80% or 90% for specific frequency mismatches, which is otherwise attainable in static cascaded systems. This result indicates that by carefully adjusting the angular velocities of such spinning devices, one can create nearly ideal remote entanglement between nonidentical mechanical oscillators. More importantly, it is stressed that our numerical calculations of  $E_N$  with respect to frequency-mismatched oscillators is performed without any parameter constraints required by the RWA approximation, which could facilitate the achievement of such entanglement between nonidentical mechanical oscillators within the current optical-wavelength COM devices.

After having established the nonreciprocal entanglement, we now investigate the associated nonreciprocal quadrature statistics of the two relevant nonidentical mechanical oscillators. For this purpose, we plot a selection of characteristic projections of the reconstructed Wigner function  $W(\psi)$  and their corresponding CM  $V_{\mu\nu}$  in Fig. 4. Here, as a specific example, we have taken  $\Delta/\omega_{m,l} = 0.68$  and  $\chi = 0.95$ , while the other parameters are chosen as the same in Fig. 3. Because the steady state of this compound system belongs to the class of Gaussian state, its reconstructed Wigner function  $W(\psi)$  can thus be characterized by a multivariate normal distribution, which is defined as

$$W(\psi) = \frac{\exp\left[-\frac{1}{2}(\psi^\dagger V_{\mu\nu}^{-1} \psi)\right]}{\pi^2 \sqrt{\det(V_{\mu\nu})}}. \quad (23)$$

Figures 4(a) and 4(b) demonstrate the characteristic projections of  $W(\psi)$  on two-dimensional subspaces with respect to the left and right input directions, respectively, along with that of an ideal vacuum state for reference. The ellipse (circle) with solid (dashed) line indicates a drop by  $1/e$  of the maximum value of  $W(\psi)$  for the relevant steady (vacuum) state of this compound system. When the boundary of the ellipse enters the circle, it indicates a situation where the variance of the relevant state is smaller than that of a vacuum state, and thus such state is a squeezed state. In case of the left input direction, it is found that the reconstructed Wigner function  $W(\psi)$  could exhibit all typical features of an entangled state: (i) the projections of  $W(\psi)$  for local quadrature pairs of each single mechanical oscillator is consistent with a Gaussian distribution of large variance, resulting from the phase-preserving amplification of vacuum state [see left column of Fig. 4(a)]; (ii) the projection of  $W(\psi)$  for cross-quadrature pairs, e.g.,  $\{p_l, q_r\}$  or  $\{q_l, p_r\}$ , is squeezed along the diagonal direction, indicating the emergence of two-mode squeezing correlations between the associated mechanical oscillators [see middle and right column of Fig. 4(a)]. In contrast, for the right input direction, it is found that none of the characteristic projections of  $W(\psi)$  show squeezing correlation for quadrature pairs [see Fig. 4(b)]. These results are consistent with the features of the nonreciprocal entanglement previously shown in Fig. 3. Besides, as seen in Fig. 4(c), the corresponding CM  $V_{\mu\nu}$  with respect to the left and right input directions are both characterized by four dominant diagonal elements and eight minor off-diagonal elements, with  $V_{13} \approx V_{24}$ ,  $V_{14} \approx -V_{23}$ ,  $V_{31} \approx V_{42}$  and  $V_{32} \approx -V_{41}$ , which clearly display the correlations and anticorrelations between the cross-quadrature pairs. Also, from these results, one can find that the correlations of cross-quadrature pairs for the case of right input direction is smaller than that of its left-input counterparts, which is one of the possible reasons

for the achievement of nonreciprocal entanglement in the previous discussions.

Finally, we remark that by utilizing a single spinning COM resonator, we have proposed how to achieve nonreciprocal entanglement between optical field and mechanical motion very recently, and revealed its counterintuitive property as being robust against random losses [93]. In this paper, we mainly focus on the generation and manipulation of nonreciprocal entanglement between two massive mechanical oscillators and investigate how to enhance the degree of such entanglement by exploiting the nonreciprocal control of a cascaded system.

#### IV. CONCLUSION

In summary, we have presented an effective method to generate and manipulate nonreciprocal entanglement between two spatially separated mechanical oscillators in a cascaded COM system, and reveal its unique properties by which one can entangle two frequency-mismatched mechanical oscillators through a single-tone driving laser with considerable entanglement degrees, which are otherwise inaccessible in conventional cascaded COM systems. The Sagnac effect induced by spinning devices played a key role in our proposed scheme. It allowed us to break the time reversal symmetry of this compound system, and also to optimize the optical-radiation-pressure mediated interactions between mechanical oscillators. As a result, by selectively spinning the WGM resonators, we observed the achievement of nonreciprocal entanglement, and more excitingly, the enhancement of such entanglement between two nonidentical mechanical oscillators. Besides, we also found that the quadrature statics of the associated mechanical oscillators is simultaneously nonreciprocal as well, that is, the two-mode squeezing cor-

relations for cross-quadrature pairs is present merely with regards to one specific input direction. These findings, combining the concepts of nonreciprocal physics [52–54] and quantum states engineering [1–3, 21, 51], provide an enticing new opportunity to generate, manipulate and harness the macroscopic entanglement between distinct massive mechanical objects [39–50]. Furthermore, we also envision that, instead of using spinning devices as described here, future developments with the engineering of nonreciprocal quantum entanglement can also be implemented based on varieties of other nonreciprocal devices that involve atomic ensembles [56–58], nonlinear optical cavities [59–63], COM systems [64–67], and synthetic structures [68–71]. As such, in a broader view, we believe that our proposed scheme is poised to serve as a useful tool for conceptually exploration of quantum fundamental theories [1], facilitate the manipulation of various kinds of couplings between remote quantum systems within cascaded configurations [94–97], and provide appealing quantum resources for emerging quantum technologies ranging from quantum information processing [2, 3, 51] to quantum sensing [4].

#### V. ACKNOWLEDGMENT

The authors thank Jie-Qiao Liao and Xun-Wei Xu for helpful discussions. H. J. is supported by the National Natural Science Foundation of China (NSFC, Grants No. 11935006 and 11774086) and the Science and Technology Innovation Program of Hunan Province (Grant No. 2020RC4047). L.-M. K. is supported by the NSFC (Grants No. 1217050862, 11935006 and 11775075). Y.-F. J. is supported by the NSFC (Grant No. 12147156), the China Postdoctoral Science Foundation (Grants No. 2021M701176 and 2022T150208) and the Science and Technology Innovation Program of Hunan Province (Grant No. 2021RC2078).

---

[1] R. Horodecki, P. Horodecki, M. Horodecki, and K. Horodecki, Quantum entanglement, *Rev. Mod. Phys.* **81**, 865 (2009).

[2] U. L. Andersen, G. Leuchs, and C. Silberhorn, Continuous-variable quantum information processing, *Laser & Photon. Rev.* **4**, 337 (2010).

[3] M. A. Nielsen and I. L. Chuang, *Quantum Computation and Quantum Information* (Cambridge University Press, Cambridge, UK, 2010).

[4] C. L. Degen, F. Reinhard, and P. Cappellaro, Quantum sensing, *Rev. Mod. Phys.* **89**, 035002 (2017).

[5] J. P. Dowling and G. J. Milburn, Quantum technology: the second quantum revolution, *Phil. Trans. R. Soc. A* **361**, 1655 (2003).

[6] J. M. Raimond, M. Brune, and S. Haroche, Manipulating quantum entanglement with atoms and photons in a cavity, *Rev. Mod. Phys.* **73**, 565 (2001).

[7] J.-W. Pan, Z.-B. Chen, C.-Y. Lu, H. Weinfurter, A. Zeilinger, and M. Żukowski, Multiphoton entanglement and interferometry, *Rev. Mod. Phys.* **84**, 777 (2012).

[8] N. Friis, G. Vitagliano, M. Malik, and M. Huber, Entanglement certification from theory to experiment, *Nat. Rev. Phys.* **1**, 72 (2019).

[9] X.-C. Yao, T.-X. Wang, P. Xu, H. Lu, G.-S. Pan, X.-H. Bao, C.-Z. Peng, C.-Y. Lu, Y.-A. Chen, and J.-W. Pan, Observation of eight-photon entanglement, *Nat. Photonics* **6**, 225 (2012).

[10] X.-L. Wang, L.-K. Chen, W. Li, H.-L. Huang, C. Liu, C. Chen, Y.-H. Luo, Z.-E. Su, D. Wu, Z.-D. Li, H. Lu, Y. Hu, X. Jiang, C.-Z. Peng, L. Li, N.-L. Liu, Y.-A. Chen, C.-Y. Lu, and J.-W. Pan, Experimental Ten-Photon Entanglement, *Phys. Rev. Lett.* **117**, 210502 (2016).

[11] H. Häffner, W. Hänsel, C. F. Roos, J. Benhelm, D. Chek-al-kar, M. Chwalla, T. Körber, U. D. Rapol, M. Riebe, P. O. Schmidt, C. Becher, O. Gühne, W. Dür, R. Blatt, Scalable multiparticle entanglement of trapped ions, *Nature (London)* **438**, 643 (2005).

[12] A. Stute, B. Casabone, P. Schindler, T. Monz, P. O. Schmidt, B. Brandstaetter, T. E. Northup, and R. Blatt, Tunable ion-photon entanglement in an optical cavity, *Nature (London)* **485**, 482 (2012).

[13] H.-N. Dai, B. Yang, A. Reingruber, X.-F. Xu, X. Jiang, Y.-A. Chen, Z.-S. Yuan, and J.-W. Pan, Generation and detection of atomic spin entanglement in optical lattices, *Nat. Phys.* **12**, 783 (2016).

[14] T. M. Karg, B. Gouraud, C. T. Ngai, G.-L. Schmid, K. Hammerer, and P. Treutlein, Light-mediated strong coupling between a mechanical oscillator and atomic spins 1 meter apart, *Science* **369**, 174 (2020).

[15] X.-Y. Luo, Y. Yu, J.-L. Liu, M.-Y. Zheng, C.-Y. Wang, B. Wang, J. Li, X. Jiang, X.-P. Xie, Q. Zhang, X.-H. Bao, and J.-W. Pan, Postselected Entanglement between Two Atomic Ensembles Separated by 12.5 km, *Phys. Rev. Lett.* **129**,

050503 (2022).

[16] P. Campagne-Ibarcq, E. Zalys-Geller, A. Narla, S. Shankar, P. Reinhold, L. Burkhardt, C. Axline, W. Pfaff, L. Frunzio, R. J. Schoelkopf, and M. H. Devoret, Deterministic Remote Entanglement of Superconducting Circuits through Microwave Two-Photon Transitions, *Phys. Rev. Lett.* **120**, 200501 (2018).

[17] P. Kurpiers, P. Magnard, T. Walter, B. Royer, M. Pechal, J. Heinsoo, Y. Salathé, A. Akin, S. Storz, J.-C. Besse, S. Gasparinetti, A. Blais, and A. Wallraff, Deterministic quantum state transfer and remote entanglement using microwave photons, *Nature (London)* **558**, 264 (2018).

[18] T. van Leent, M. Bock, F. Fertig, R. Garthoff, S. Eppelt, Y. Zhou, P. Malik, M. Seubert, T. Bauer, W. Rosenfeld, C. Becher, and H. Weinfurter, Entangling single atoms over 33 km telecom fibre, *Nature (London)* **607**, 69 (2022).

[19] M. Aspelmeyer, T. J. Kippenberg, and F. Marquardt, Cavity optomechanics, *Rev. Mod. Phys.* **86**, 1391 (2014).

[20] H. Xiong, L.-G. Si, X.-Y. Lü, X.-X. Yang, and Y. Wu, Review of cavity optomechanics in the weak-coupling regime: from linearization to intrinsic nonlinear interactions, *Sci. China Phys. Mech. Astron.* **58**, 1 (2015).

[21] S. Barzanjeh, A. Xuereb, S. Gröblacher, M. Paternostro, C. A. Regal, and E. M. Weig, Optomechanics for quantum technologies, *Nat. Phys.* **18**, 15 (2022).

[22] A. D. O'Connell, M. Hofheinz, M. Ansmann, R. C. Bialczak, M. Lenander, E. Lucero, M. Neeley, D. Sank, H. Wang, M. Weides, J. Wenner, J. M. Martinis, and A. N. Cleland, Quantum ground state and single-phonon control of a mechanical resonator, *Nature (London)* **464**, 697 (2010).

[23] D.-G. Lai, F. Zou, B.-P. Hou, Y.-F. Xiao, and J.-Q. Liao, Simultaneous cooling of coupled mechanical resonators in cavity optomechanics, *Phys. Rev. A* **98**, 023860 (2018).

[24] K. Jähne, C. Genes, K. Hammerer, M. Wallquist, E. S. Polzik, and P. Zoller, Cavity-assisted squeezing of a mechanical oscillator, *Phys. Rev. A* **79**, 063819 (2009).

[25] E. E. Wollman, C. U. Lei, A. J. Weinstein, J. Suh, A. Kronwald, F. Marquardt, A. A. Clerk, and K. C. Schwab, Quantum squeezing of motion in a mechanical resonator, *Science* **349**, 952 (2015).

[26] H. Xie, C.-G. Liao, X. Shang, M.-Y. Ye, and X.-M. Lin, Phonon blockade in a quadratically coupled optomechanical system, *Phys. Rev. A* **96**, 013861 (2017).

[27] J.-Q. Liao and L. Tian, Macroscopic Quantum Superposition in Cavity Optomechanics, *Phys. Rev. Lett.* **116**, 163602 (2016).

[28] H. Yu, L. McCuller, M. Tse, N. Kijbunchoo, L. Barsotti, N. Mavalvala, and L. S. Collaboration, Quantum correlations between light and the kilogram-mass mirrors of LIGO, *Nature (London)* **583**, 43 (2020).

[29] E. Verhagen, S. Deléglise, S. Weis, A. Schliesser, and T. J. Kippenberg, Quantum-coherent coupling of a mechanical oscillator to an optical cavity mode, *Nature (London)* **482**, 63 (2012).

[30] D. Vitali, S. Gigan, A. Ferreira, H. R. Böhm, P. Tombesi, A. Guerreiro, V. Vedral, A. Zeilinger, and M. Aspelmeyer, Optomechanical Entanglement between a Movable Mirror and a Cavity Field, *Phys. Rev. Lett.* **98**, 030405 (2007).

[31] T. A. Palomaki, J. D. Teufel, R. W. Simmonds, and K. W. Lehnert, Entangling Mechanical Motion with Microwave Fields, *Science* **342**, 710 (2013).

[32] R. Ghobadi, S. Kumar, B. Pepper, D. Bouwmeester, A. I. Lvovsky, and C. Simon, Optomechanical Micro-Macro Entanglement, *Phys. Rev. Lett.* **112**, 080503 (2014).

[33] R. Riedinger, S. Hong, R. A. Norte, J. A. Slater, J. Shang, A. G. Krause, V. Anant, M. Aspelmeyer, and S. Gröblacher, Non-classical correlations between single photons and phonons from a mechanical oscillator, *Nature (London)* **530**, 313 (2016).

[34] I. Marinković, A. Wallucks, R. Riedinger, S. Hong, M. Aspelmeyer, and S. Gröblacher, Optomechanical Bell Test, *Phys. Rev. Lett.* **121**, 220404 (2018).

[35] Y. Li, Y.-F. Jiao, J.-X. Liu, A. Miranowicz, Y.-L. Zuo, L.-M. Kuang, and H. Jing, Vector optomechanical entanglement, *Nanophotonics* **11**, 67 (2022).

[36] H. Tan and G. Li, Multicolor quadripartite entanglement from an optomechanical cavity, *Phys. Rev. A* **84**, 024301 (2011).

[37] S. Barzanjeh, E. S. Redchenko, M. Peruzzo, M. Wulf, D. P. Lewis, G. Arnold, and J. M. Fink, Stationary entangled radiation from micromechanical motion, *Nature (London)* **570**, 480 (2019).

[38] J. Chen, M. Rossi, D. Mason, and A. Schliesser, Entanglement of propagating optical modes via a mechanical interface, *Nat. Commun.* **11**, 943 (2020).

[39] S. Mancini, V. Giovannetti, D. Vitali, and P. Tombesi, Entangling Macroscopic Oscillators Exploiting Radiation Pressure, *Phys. Rev. Lett.* **88**, 120401 (2002).

[40] S. Mancini, D. Vitali, V. Giovannetti, and P. Tombesi, Stationary entanglement between macroscopic mechanical oscillators, *Eur. Phys. J. D* **22**, 417 (2003).

[41] S. Huang and G. S. Agarwal, Entangling nanomechanical oscillators in a ring cavity by feeding squeezed light, *New J. Phys.* **11**, 103044 (2009).

[42] H. Tan, L. F. Buchmann, H. Seok, and G. Li, Achieving steady-state entanglement of remote micromechanical oscillators by cascaded cavity coupling, *Phys. Rev. A* **87**, 022318 (2013).

[43] J.-Q. Liao, Q.-Q. Wu, and F. Nori, Entangling two macroscopic mechanical mirrors in a two-cavity optomechanical system, *Phys. Rev. A* **89**, 014302 (2014).

[44] C.-J. Yang, J.-H. An, W. Yang, and Y. Li, Generation of stable entanglement between two cavity mirrors by squeezed-reservoir engineering, *Phys. Rev. A* **92**, 062311 (2015).

[45] J. Li, I. M. Haghghi, N. Malossi, S. Zippilli, and D. Vitali, Generation and detection of large and robust entanglement between two different mechanical resonators in cavity optomechanics, *New J. Phys.* **17**, 103037 (2015).

[46] D.-G. Lai, J.-Q. Liao, A. Miranowicz, and F. Nori, Noise-Tolerant Optomechanical Entanglement via Synthetic Magnetism, *Phys. Rev. Lett.* **129**, 063602 (2022).

[47] R. Riedinger, A. Wallucks, I. Marinković, C. Löschnauer, M. Aspelmeyer, S. Hong, and S. Gröblacher, Remote quantum entanglement between two micromechanical oscillators, *Nature (London)* **556**, 473 (2018).

[48] C. F. Ockeloen-Korppi, E. Damskägg, J.-M. Pirkkalainen, M. Asjad, A. A. Clerk, F. Massel, M. J. Woolley, and M. A. Sillanpää, Stabilized entanglement of massive mechanical oscillators, *Nature (London)* **556**, 478 (2018).

[49] S. Kotler, G. A. Peterson, E. Shojaee, F. Lecocq, K. Cicak, A. Kwiatkowski, S. Geller, S. Glancy, E. Knill, R. W. Simmonds, J. Aumentado, and J. D. Teufel, Direct observation of deterministic macroscopic entanglement, *Science* **372**, 622 (2021).

[50] L. Mercier de Lépinay, C. F. Ockeloen-Korppi, M. J. Woolley, and M. A. Sillanpää, Quantum mechanics-free subsystem with mechanical oscillators, *Science* **372**, 625 (2021).

[51] F. Flamini, N. Spagnolo, and F. Sciarrino, Photonic quantum information processing: a review, *Rep. Prog. Phys.* **82**, 016001

(2018).

[52] D. L. Sounas and A. Alù, Non-reciprocal photonics based on time modulation, *Nat. Photonics* **11**, 774 (2017).

[53] P. Lodahl, S. Mahmoodian, S. Stobbe, A. Rauschenbeutel, P. Schneeweiss, J. Volz, H. Pichler, and P. Zoller, Chiral quantum optics, *Nature (London)* **541**, 473 (2017).

[54] C. Caloz, A. Alù, S. Tretyakov, D. Sounas, K. Achouri, and Z.-L. Deck-Léger, Electromagnetic Nonreciprocity, *Phys. Rev. Applied* **10**, 047001 (2018).

[55] Y. Shoji and T. Mizumoto, Magneto-optical non-reciprocal devices in silicon photonics, *Sci. Technol. Adv. Mater.* **15**, 014602 (2014).

[56] S. Zhang, Y. Hu, G. Lin, Y. Niu, K. Xia, J. Gong, and S. Gong, Thermal-motion-induced non-reciprocal quantum optical system, *Nat. Photonics* **12**, 744 (2018).

[57] P. Yang, X. Xia, H. He, S. Li, X. Han, P. Zhang, G. Li, P. Zhang, J. Xu, Y. Yang, and T. Zhang, Realization of Nonlinear Optical Nonreciprocity on a Few-Photon Level Based on Atoms Strongly Coupled to an Asymmetric Cavity, *Phys. Rev. Lett.* **123**, 233604 (2019).

[58] C. Liang, B. Liu, A.-N. Xu, X. Wen, C. Lu, K. Xia, M. K. Tey, Y.-C. Liu, and L. You, Collision-Induced Broadband Optical Nonreciprocity, *Phys. Rev. Lett.* **125**, 123901 (2020).

[59] C.-H. Dong, Z. Shen, C.-L. Zou, Y.-L. Zhang, W. Fu, and G.-C. Guo, Brillouin-scattering-induced transparency and non-reciprocal light storage, *Nat. Commun.* **6**, 6193 (2015).

[60] J. Kim, M. C. Kuzyk, K. Han, H. Wang, and G. Bahl, Non-reciprocal Brillouin scattering induced transparency, *Nat. Phys.* **11**, 275 (2015).

[61] K. Xia, F. Nori, and M. Xiao, Cavity-Free Optical Isolators and Circulators Using a Chiral Cross-Kerr Nonlinearity, *Phys. Rev. Lett.* **121**, 203602 (2018).

[62] A. Rosario Hamann, C. Müller, M. Jerger, M. Zanner, J. Combes, M. Pletyukhov, M. Weides, T. M. Stace, and A. Fedorov, Nonreciprocity Realized with Quantum Nonlinearity, *Phys. Rev. Lett.* **121**, 123601 (2018).

[63] L. Tang, J. Tang, M. Chen, F. Nori, M. Xiao, and K. Xia, Quantum Squeezing Induced Optical Nonreciprocity, *Phys. Rev. Lett.* **128**, 083604 (2022).

[64] S. Manipatruni, J. T. Robinson, and M. Lipson, Optical Nonreciprocity in Optomechanical Structures, *Phys. Rev. Lett.* **102**, 213903 (2009).

[65] Z. Shen, Y.-L. Zhang, Y. Chen, C.-L. Zou, Y.-F. Xiao, X.-B. Zou, F.-W. Sun, G.-C. Guo, and C.-H. Dong, Experimental realization of optomechanically induced non-reciprocity, *Nat. Photonics* **10**, 657 (2016).

[66] N. R. Bernier, L. D. Tóth, A. Koottandavida, M. A. Ioannou, D. Malz, A. Nunnenkamp, A. K. Feofanov, and T. J. Kippenberg, Nonreciprocal reconfigurable microwave optomechanical circuit, *Nat. Commun.* **8**, 604 (2017).

[67] L. Mercier de Lépinay, E. Damskägg, C. F. Ockeloen-Korppi, and M. A. Sillanpää, Realization of Directional Amplification in a Microwave Optomechanical Device, *Phys. Rev. Applied* **11**, 034027 (2019).

[68] B. Peng, S. K. Özdemir, F. Lei, F. Monifi, M. Gianfreda, G. L. Long, S. Fan, F. Nori, C. M. Bender, and L. Yang, Parity-time-symmetric whispering-gallery microcavities, *Nat. Phys.* **10**, 394 (2014).

[69] L. Chang, X. Jiang, S. Hua, C. Yang, J. Wen, L. Jiang, G. Li, G. Wang, and M. Xiao, Parity-time symmetry and variable optical isolation in active-passive-coupled microresonators, *Nat. Photonics* **8**, 524 (2014).

[70] X.-W. Xu, Y. Li, B. Li, H. Jing, and A.-X. Chen, Nonreciprocity via Nonlinearity and Synthetic Magnetism, *Phys. Rev. Applied* **13**, 044070 (2020).

[71] Y. Chen, Y.-L. Zhang, Z. Shen, C.-L. Zou, G.-C. Guo, and C.-H. Dong, Synthetic Gauge Fields in a Single Optomechanical Resonator, *Phys. Rev. Lett.* **126**, 123603 (2021).

[72] D.-W. Wang, H.-T. Zhou, M.-J. Guo, J.-X. Zhang, J. Evers, and S.-Y. Zhu, Optical Diode Made from a Moving Photonic Crystal, *Phys. Rev. Lett.* **110**, 093901 (2013).

[73] H. Lü, Y. Jiang, Y.-Z. Wang, and H. Jing, Optomechanically induced transparency in a spinning resonator, *Photon. Res.* **5**, 367 (2017).

[74] S. Maayani, R. Dahan, Y. Kligerman, E. Moses, A. U. Hassan, H. Jing, F. Nori, D. N. Christodoulides, and T. Carmon, Flying couplers above spinning resonators generate irreversible refraction, *Nature (London)* **558**, 569 (2018).

[75] Z. Lin, H. Ramezani, T. Eichelkraut, T. Kottos, H. Cao, and D. N. Christodoulides, Unidirectional Invisibility Induced by  $\mathcal{PT}$ -Symmetric Periodic Structures, *Phys. Rev. Lett.* **106**, 213901 (2011).

[76] B. Bahari, A. Ndaa, F. Vallini, A. El Amili, Y. Fainman, and B. Kanté, Nonreciprocal lasing in topological cavities of arbitrary geometries, *Science* **358**, 636 (2017).

[77] S. Kim, J. M. Taylor, and G. Bahl, Dynamic suppression of Rayleigh backscattering in dielectric resonators, *Optica* **6**, 1016 (2019).

[78] D.-W. Zhang, L.-L. Zheng, C. You, C.-S. Hu, Y. Wu, and X.-Y. Lü, Nonreciprocal chaos in a spinning optomechanical resonator, *Phys. Rev. A* **104**, 033522 (2021).

[79] B. Li, S. K. Özdemir, X.-W. Xu, L. Zhang, L.-M. Kuang, and H. Jing, Nonreciprocal optical solitons in a spinning Kerr resonator, *Phys. Rev. A* **103**, 053522 (2021).

[80] Y. Jiang, S. Maayani, T. Carmon, F. Nori, and H. Jing, Nonreciprocal Phonon Laser, *Phys. Rev. Applied* **10**, 064037 (2018).

[81] K.-W. Huang, Y. Wu, and L.-G. Si, Parametric-amplification-induced nonreciprocal magnon laser, *Opt. Lett.* **47**, 3311 (2022).

[82] W.-A. Li, G.-Y. Huang, J.-P. Chen, and Y. Chen, Nonreciprocal enhancement of optomechanical second-order sidebands in a spinning resonator, *Phys. Rev. A* **102**, 033526 (2020).

[83] Y. Shen, M. Bradford, and J.-T. Shen, Single-Photon Diode by Exploiting the Photon Polarization in a Waveguide, *Phys. Rev. Lett.* **107**, 173902 (2011).

[84] M.-X. Dong, K.-Y. Xia, W.-H. Zhang, Y.-C. Yu, Y.-H. Ye, E.-Z. Li, L. Zeng, D.-S. Ding, B.-S. Shi, G.-C. Guo, and F. Nori, All-optical reversible single-photon isolation at room temperature, *Sci. Adv.* **7**, eabe8924 (2021).

[85] S.-Y. Ren, W. Yan, L.-T. Feng, Y. Chen, Y.-K. Wu, X.-Z. Qi, X.-J. Liu, Y.-J. Cheng, B.-Y. Xu, L.-J. Deng, G.-C. Guo, L. Bi, and X.-F. Ren, Single-Photon Nonreciprocity with an Integrated Magneto-Optical Isolator, *Laser & Photon. Rev.* **16**, 2100595 (2022).

[86] M. Scheucher, A. Hilico, E. Will, J. Volz, and A. Rauschenbeutel, Quantum optical circulator controlled by a single chirally coupled atom, *Science* **354**, 1577 (2016).

[87] J.-S. Tang, W. Nie, L. Tang, M. Chen, X. Su, Y. Lu, F. Nori, and K. Xia, Nonreciprocal Single-Photon Band Structure, *Phys. Rev. Lett.* **128**, 203602 (2022).

[88] S. Barzanjeh, M. Aquilina, and A. Xuereb, Manipulating the Flow of Thermal Noise in Quantum Devices, *Phys. Rev. Lett.* **120**, 060601 (2018).

[89] R. Huang, A. Miranowicz, J.-Q. Liao, F. Nori, and H. Jing, Nonreciprocal Photon Blockade, *Phys. Rev. Lett.* **121**, 153601 (2018).

[90] B. Li, R. Huang, X. Xu, A. Miranowicz, and H. Jing, Nonreciprocal unconventional photon blockade in a spinning op-

tomechanical system, *Photon. Res.* **7**, 630 (2019).

[91] P. Yang, M. Li, X. Han, H. He, G. Li, C.-L. Zou, P. Zhang, and T. Zhang, Non-reciprocal cavity polariton, [arXiv:1911.10300](https://arxiv.org/abs/1911.10300).

[92] Y. Wang, W. Xiong, Z. Xu, G.-Q. Zhang, and J.-Q. You, Dissipation-induced nonreciprocal magnon blockade in a magnon-based hybrid system, *Sci. China Phys. Mech. Astron.* **65**, 260314 (2022).

[93] Y.-F. Jiao, S.-D. Zhang, Y.-L. Zhang, A. Miranowicz, L.-M. Kuang, and H. Jing, Nonreciprocal Optomechanical Entanglement against Backscattering Losses, *Phys. Rev. Lett.* **125**, 143605 (2020).

[94] Y.-F. Xiao, M. Li, Y.-C. Liu, Y. Li, X. Sun, and Q. Gong, Asymmetric Fano resonance analysis in indirectly coupled microresonators, *Phys. Rev. A* **82**, 065804 (2010).

[95] T. Li, T.-Y. Bao, Y.-L. Zhang, C.-L. Zou, X.-B. Zou, and G.-C. Guo, Long-distance synchronization of unidirectionally cascaded optomechanical systems, *Opt. Express* **24**, 12336 (2016).

[96] E. Gil-Santos, M. Labousse, C. Baker, A. Goetschy, W. Hease, C. Gomez, A. Lemaître, G. Leo, C. Ciuti, and I. Favero, Light-Mediated Cascaded Locking of Multi-ple Nano-Optomechanical Oscillators, *Phys. Rev. Lett.* **118**, 063605 (2017).

[97] J. Li, Z.-H. Zhou, S. Wan, Y.-L. Zhang, Z. Shen, M. Li, C.-L. Zou, G.-C. Guo, and C.-H. Dong, All-Optical Synchronization of Remote Optomechanical Systems, *Phys. Rev. Lett.* **129**, 063605 (2022).

[98] H. Qin, Y. Yin, and M. Ding, Spinning indirectly coupled optical resonators, *Appl. Phys. Express* **14**, 012002 (2020).

[99] G. B. Malykin, The Sagnac effect: correct and incorrect explanations, *Phys. Usp.* **43**, 1229 (2000).

[100] C. W. Gardiner and P. Zoller, *Quantum Noise* (Springer, Berlin, 2000).

[101] E. X. DeJesus and C. Kaufman, Routh-Hurwitz criterion in the examination of eigenvalues of a system of nonlinear ordinary differential equations, *Phys. Rev. A* **35**, 5288 (1987).

[102] G. Adesso, A. Serafini, and F. Illuminati, Extremal entanglement and mixedness in continuous variable systems, *Phys. Rev. A* **70**, 022318 (2004).

[103] R. Simon, Peres-Horodecki Separability Criterion for Continuous Variable Systems, *Phys. Rev. Lett.* **84**, 2726 (2000).